

Article

Geospatial Network Analysis and Origin-Destination Clustering of Bike-Sharing Activities during the COVID-19 Pandemic

Rui Xin ¹, Linfang Ding ², Bo Ai ¹, Min Yang ^{3,*} , Ruoxin Zhu ⁴ , Bin Cao ⁵ and Liqiu Meng ⁶

¹ College of Geodesy and Geomatics, Shandong University of Science and Technology, Qingdao 266590, China

² Department of Civil and Environmental Engineering, Norwegian University of Science and Technology, 7034 Trondheim, Norway

³ School of Resource and Environment Sciences, Wuhan University, Wuhan 430072, China

⁴ State Key Laboratory of Geo-Information Engineering, Xi'an Research Institute of Surveying and Mapping, Xi'an 710054, China

⁵ Shandong Provincial No. 4 Institute of Geological and Mineral Survey, Weifang 261021, China

⁶ Chair of Cartography and Visual Analytics, Technical University of Munich, 80333 Munich, Germany

* Correspondence: yangmin2003@whu.edu.cn; Tel.: +86-138-7117-6133

Abstract: Bike-sharing data are an important data source to study urban mobility in the context of the coronavirus disease 2019 (COVID-19). However, studies that focus on different bike-sharing activities including both riding and rebalancing are sparse. This limits the comprehensiveness of the analysis of the impact of the pandemic on bike-sharing. In this study, we combine geospatial network analysis and origin-destination (OD) clustering methods to explore the spatiotemporal change patterns hidden in the bike-sharing data during the pandemic. Different from previous research that mostly focuses on the analysis of riding behaviors, we also extract and analyze the rebalancing data of a bike-sharing system. In this study, we propose a framework including three components: (1) a geospatial network analysis component for a statistical and spatiotemporal description of the overall riding flows and behaviors, (2) an origin-destination clustering component that compensates the network analysis by identifying large flow groups in which individual edges start from and end at nearby stations, and (3) a rebalancing data analysis component for the understanding of the rebalancing patterns during the pandemic. We test our framework using bike-sharing data collected in New York City. The results show that the spatial distribution of the main riding flows changed significantly in the pandemic compared to pre-pandemic time. For example, many riding trips seemed to expand the purposes of riding for work-home commuting to more leisure activities. Furthermore, we found that the changes in the riding flow patterns led to changes in the spatiotemporal distributions of bike rebalancing, such as the shifting of the rebalancing peak time and the increased ratio between the number of rebalancing and the total number of rides. Policy implications are also discussed based on our findings.

Keywords: COVID-19; bike-sharing data; spatiotemporal change detection; geospatial network; origin-destination clustering



Citation: Xin, R.; Ding, L.; Ai, B.; Yang, M.; Zhu, R.; Cao, B.; Meng, L. Geospatial Network Analysis and Origin-Destination Clustering of Bike-Sharing Activities during the COVID-19 Pandemic. *ISPRS Int. J. Geo-Inf.* **2023**, *12*, 23. <https://doi.org/10.3390/ijgi12010023>

Academic Editors: Wolfgang Kainz and Hartwig H. Hochmair

Received: 20 November 2022

Revised: 6 January 2023

Accepted: 7 January 2023

Published: 13 January 2023



Copyright: © 2023 by the authors. Licensee MDPI, Basel, Switzerland. This article is an open access article distributed under the terms and conditions of the Creative Commons Attribution (CC BY) license (<https://creativecommons.org/licenses/by/4.0/>).

1. Introduction

The emergence and rapid spread of coronavirus disease 2019 (COVID-19) seriously affected not only individuals' daily lives, work, and social interactions, but also the global economy [1], politics [2], and the environment [3]. Human activities are an important driving factor in the spread of the virus because the virus can be easily transmitted from person to person. Different measures were taken to control the spread of the virus, for example, individuals took self-protection actions by reducing their travels and maintaining social distance and self-isolation, and governments enacted lockdown policies and travel restrictions. All of these measures inevitably affect people's mobility.

People's travel activities constitute an important part of the mobility flow in the city. Bike riding is promoted as a low-carbon, environmentally friendly, and healthy travel mode [4]. As a result, more and more people choose to ride for both commuting and leisure activities. In the era of sharing economy, bike-sharing became a convenient transport means in cities [5]. Many electric-based bike-sharing systems appeared and were promoted, further promoting environmental protection and convenient transportation [6]. With the development of information communication technologies, bike-sharing data are increasingly collected, often with spatial and temporal properties reflecting the usage of bikes. This rich amount of data provides a new perspective for studying urban human mobility and received considerable attention in recent years [7,8]. In this context, employing bike-sharing data to explore human mobility and spatial interactions in cities is beneficial for understanding the urban dynamics during the pandemic [9,10]. Many researchers explored the impact of the COVID-19 pandemic on bike-sharing in different places worldwide, such as in North America [11], Asia [12,13], and Europe [14].

Bike-sharing riding data are a typical kind of origin-destination (OD) data that represent movement through geographic space from starting locations to ending locations. OD data clustering is an effective way to discover spatial distribution patterns [15,16] and to extract the main features and structure flow data [17]. People's activities in the city are not evenly distributed in time and space due to reasons such as the differences in spatial planning, such as functional zoning and land use types, as well as different human daily routines, such as varying commuting and leisure time. This also leads to imbalance problems in bike-sharing systems, such as the shortage of bikes at the borrowing stations and the shortage of docks at the returning stations, which need bike rebalancing management [18,19]. The exploration of the spatiotemporal patterns of bike riding flows and their influence on bike management during the pandemic will facilitate a deeper understanding of the influence of the pandemic on human behavior, and provide support for travel planning, bike-sharing operations, and urban management. However, research on this aspect at present is still insufficient. Based on the comparative analysis of the bike-sharing data between the pre-pandemic period and the pandemic period, this study attempts to answer the following questions:

- (1) Which changes took place in the spatiotemporal patterns of main riding flows of bike-sharing during the pandemic?
- (2) How do these changes in the main riding flows influence the bike rebalancing management?

To answer the above questions, this paper proposes a framework combining methods of geospatial network analysis, OD clustering, and rebalancing data analysis. Network analysis is carried out by selecting flow and aggregation-related indicators to help understand the overall situation of the bike-sharing network. Based on the constructed network, different forms of large flow edges are analyzed. In particular, OD clustering is carried out on network edges combined with multiple constraints, such as edge flow, edge amount, distance, and angle, which aims to extract large flow edge groups and analyze their spatiotemporal distribution characteristics. In addition, the rebalancing data are extracted by continuity detection and analyzed together with riding data. We demonstrate the effectiveness of our framework using test data collected from Citi Bike in New York City. We carry out a comparative analysis of the main riding flow characteristics of bike-sharing between the pre-pandemic period and the pandemic period. Furthermore, we extract and analyze the rebalancing data to investigate the impact of the pandemic on bike dispatch management. Different from previous studies, we analyzed both riding data and rebalancing data and explored the relationship between them. This more comprehensive perspective helps provide references for different stakeholders, such as citizens, governments, and bike-sharing companies. The remainder of this paper is organized as follows: Section 2 reports related research works. Section 3 presents the study area and data. Section 4 details the main methods adopted in this study. Experiment and analysis based on Citi Bike data

are introduced in Section 5. Section 6 analyzes and discusses the results, limitations, and future works. Section 7 concludes this study.

2. Related Work

During a pandemic, emergency policies and citizen self-protection measures typically have a negative impact on mobility. The research on human mobility patterns and pandemic prediction based on movement data received a lot of attention in the context of COVID-19 [20,21]. Researchers collect movement data and study mobility patterns during the COVID-19 pandemic in a variety of ways. For instance, the traditional approach is to conduct questionnaires. König and Dreßler used telephone interviews, household surveys, and other mixed methods to study the impact of pandemics on rural mobility [22]. In addition, in combination with geographic information system (GIS) technology, a map-based online survey was applied to study the impact of the pandemic on mobility [23]. Traditional spatial data, such as remote sensing images, also play an important role in the study of mobility during the pandemic [24,25]. Various location-based multi-source data provide rich information for pandemic research [26,27].

Bike-sharing data are a typical kind of location-related data, which can be used to study human mobility during the pandemic [11,28,29]. Bike-sharing systems existed for nearly 50 years. In the past 10 years, their popularity increased dramatically worldwide [30]. Shared bikes are usually equipped with technologies such as Global Positioning System (GPS) to facilitate the system to locate their parking places [31]. Therefore, bike-sharing systems accumulate a large amount of riding data that can objectively reflect urban riding during the pandemic.

Many studies confirmed that the spread of COVID-19 and lockdown policies reduced the use of bike-sharing. For instance, the mobility of shared bikes in Beijing during the pandemic dropped by 60% compared with the same period in 2019 [32]. Hu et al. studied the data of bike-sharing in Chicago and found the proportion of commuting trips was significantly lower [9].

Researchers also found that bike-sharing riding patterns showed some new characteristics during the pandemic period. Xin et al. used a multi-scale spatial complex network to study Citi Bike data in New York and found that the aggregation of bike-sharing riding in cities decreased significantly during the pandemic period [11]. Combined with descriptive statistics methods, Teixeira and Lopes found that bike-sharing systems are resilient during a pandemic and there is a possible mode transfer of people's travel from public transportation, such as subways, to bike-sharing systems [33]. The study of the mobility of public transportation during the pandemic indicates that bikes have the smallest decline in the demand for public transportation in Budapest [34]. Compared with other public transportation modes, bikes are not enclosed and can avoid close contact between users, therefore, people are relatively more willing to use bikes during the pandemic [14]. Padmanabhan et al. conducted correlation analysis on COVID-19 cases and various bike-sharing-related variables with data from three cities and found that although bike trips decreased, the average travel time increased [35]. In addition, for safety and health reasons, biking gained new attention and became a popular leisure sport during the pandemic [36]. Based on their research findings, Jobe and Griffin called for continued bike-sharing services during the pandemic and suggested that bike-sharing operators should expand communication efforts about policies and actions to support community health [37]. Büchel et al. provided recommendations to utilize the window of opportunity for policy measures to permanently increase bike usage in response to the COVID-19 pandemic [38]. In order to facilitate citizens' healthy travel during the pandemic period, the number of bikes in European cities increased in a short term by adding temporary bike infrastructure [39].

In addition to riding, the operation of bike-sharing companies during the pandemic also deserves attention. The most typical operation is bike rebalance, which moves bikes from the stations with too many bikes to stations with too few bikes so that all stations will have enough bikes for pickup and enough docks for drop-off [18]. In terms of operation

type, rebalance can be divided into static rebalance and dynamic rebalance. Static rebalance is usually carried out at night when the riding demand is low or the system is closed. Wang and Szeto used a mixed integer linear program model to rebalance both good and broken bikes in a bike-sharing network with the minimum total CO₂ emissions [40]. A different number of transfer vehicles are involved in the rebalancing operation. Cruz et al. proposed a hybrid iterated local search algorithm that was specially designed to solve a single-vehicle static bike rebalancing problem [41]. Ho and Szeto proposed a hybrid large neighborhood search for solving the multi-vehicle rebalance problem [42]. Dynamic rebalance is mainly carried out during the daytime and takes real-time bike usage into account. Compared with static rebalance, dynamic rebalance considers more complex factors. For dock-based bike-sharing, Ghosh et al. proposed an optimization formulation to support bike repositioning and vehicle routing considering the routes for vehicles and the future expected demand of the system [43]. For dockless bike-sharing, Caggiani et al. combined spatiotemporal clusterization and nonlinear autoregressive neural networks to construct a decision support system to promote rebalance operation [44]. However, all the above studies focus on the design of the rebalance scheme. Because the rebalancing data are not generally disclosed, there are few studies on the analysis of the rebalancing data, especially on the impact of the pandemic on the rebalancing operation.

In summary, most previous studies focus on exploring riding behavior patterns and designing rebalance schemes. There is a lack of attention to the analysis of the rebalancing data. The impact of the pandemic on bike riding together with bike rebalance is not fully studied. Furthermore, the combination of different methods is limited, which affects the comprehensive analysis and representation of the results. In this study, we propose a framework consisting of geospatial network analysis and origin-destination clustering for the exploration of bike-sharing riding behaviors and the rebalancing patterns.

3. Study Area and Data

The study area of New York City in this paper is shown in Figure 1. New York City is located on the Atlantic coast of the United States. It has five districts, including Manhattan, Queens, Brooklyn, Bronx, and Staten Island, with a total area of 1214.4 square kilometers. The population of New York City is more than 8 million, making it the largest and most populous city in the United States. This world-class city directly affects the global economy, finance, and politics. The headquarters of many international organizations, multinational companies, and banks in the world, including the United Nations headquarters, are located in New York.

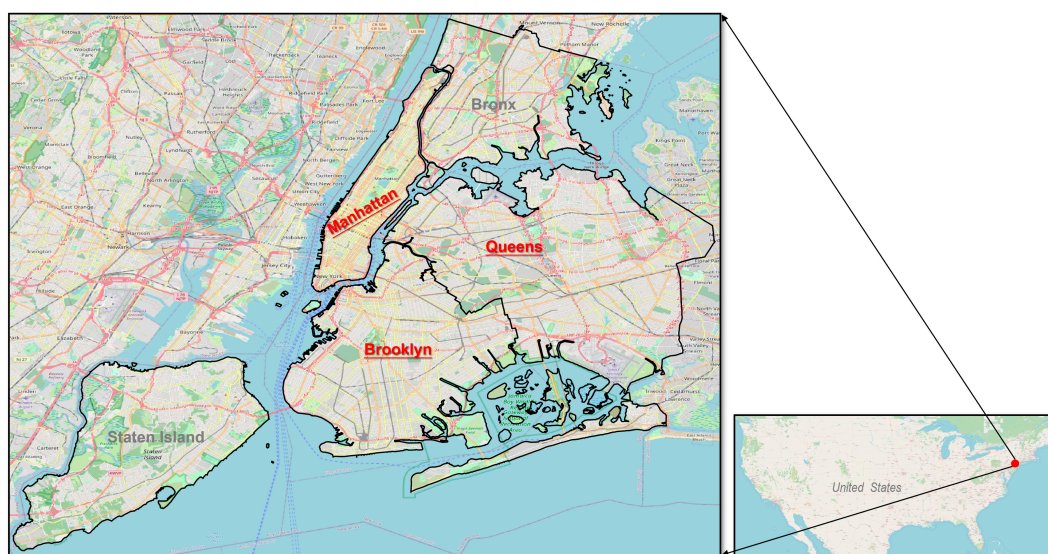


Figure 1. Study area of New York City in this study (areas with red labels have bike stations).

New York was seriously impacted during the pandemic. On 1 March 2020, New York State announced the first confirmed case of COVID-19. On 7 March, it declared a statewide emergency. On 19 March, it issued an order of “Stay at Home”, stipulating that people should not go out as far as possible except for purchasing necessary supplies, seeking medical treatment, and doing necessary work.

The data in this study are collected from Citi Bike (<https://www.citibikenyc.com/> (accessed on 6 January 2023)), a New York City public bike system, which was officially put into operation on 27 May 2013, and is the largest public bike system in the United States. It is open for use 24 h/day, 7 days/week, 365 days/year. Citi Bike is a bike-sharing system with docks. Users pick up their bikes from the start station and return them to the end station after riding. In the initial stage (2013), 6000 bikes at hundreds of stations were put into operation throughout Manhattan and Brooklyn. It announced that would double the size of the network from 6000 to 12,000 bikes just one year later. In 2016, Citi Bike gained its 100,000th annual membership. At present, Citi Bike riders take more than 100 million trips, and the main distribution of Citi Bike stations covers Manhattan, Brooklyn, and Queens, which also constitutes the study area of this study. Citi Bike releases its riding data in CSV format by month, which can be traced back to July 2013. Riding data are typical OD data, which records the spatial coordinates and attributes of the start station and the end station. At the same time, the riding information is also recorded. The attribute information and sample attribute values of the data are shown in Table 1.

Table 1. Attributes and example values of trip data.

Attributes	Example Values
Trip duration	660 (seconds)
Start station name	Graham Ave and Herbert St
Start station ID	229
Start station latitude	40.71929301
Start station longitude	−73.94500379
Start date and time	2020/4/1 0:22:35
Stop station name	W 84 St and Columbus Ave
Stop station ID	3082
Stop station latitude	40.71167351
Stop station longitude	−73.95141312
Stop date and time	2020/4/1 0:30:21
Bike ID	30,315
User type	Subscriber/customer
Gender	1 (male)/2 (female)
Year of birth	1982

4. Methodology

Our method framework is shown in Figure 2. For the trip data, we first organize it into a network form with nodes representing bike-sharing stations and edges representing riding trips. Other ride statistics are also mapped to network attribute values. Based on the above network, the overall network analysis and the OD cluster analysis are carried out. For the bike rebalancing data, we extract it through detection and organization to obtain the result in the form of OD data. Then statistical analysis and spatiotemporal analysis are carried out on the above rebalancing data.

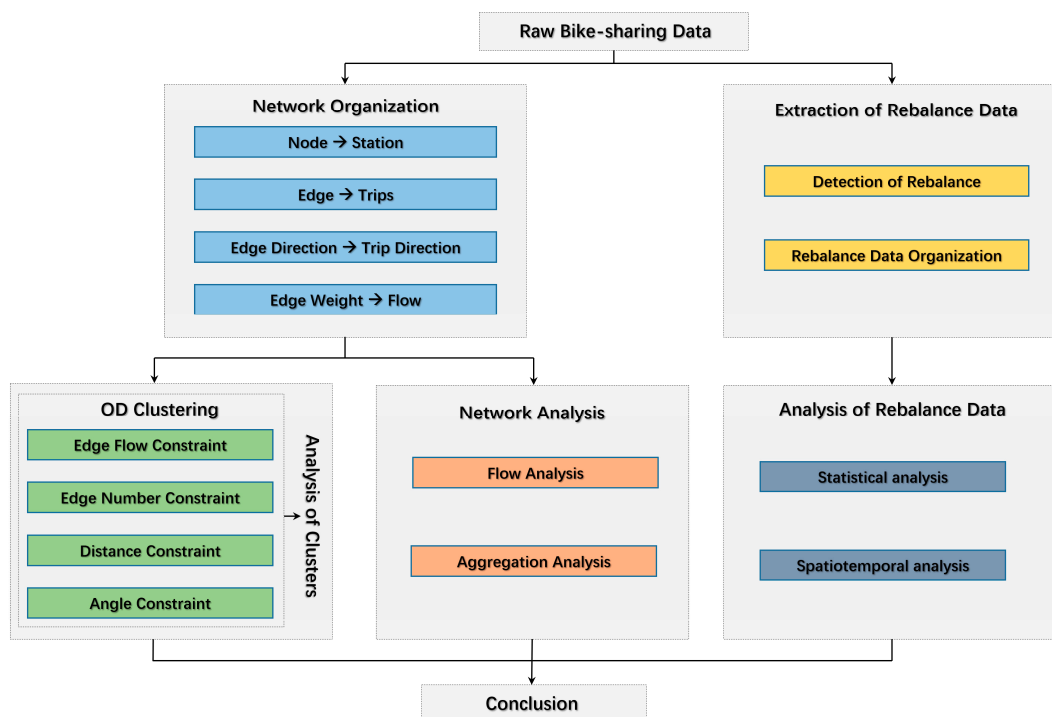


Figure 2. The method framework of our study.

4.1. Network Organization and Analysis of Bike-Sharing Data

From the raw data, we first extract the stations and riding connections between stations, as illustrated in the upper part of Figure 3. We distinguish two types of flows, i.e., station self-loop flows and inter-station flows. Station self-loop flow refers to the total number of bikes borrowed from a station and returned to the same station. Inter-station flow is the flow between two stations. This information can be structured into a network as depicted in the lower part of Figure 3, in which nodes represent stations, and directed edges represent the node inflow (i.e., the number of incoming bikes) and outflow (i.e., the number of outgoing bikes), respectively. The total flow of the station (the sum of incoming and outgoing bikes) is the total flow of the node. The higher the total flow of the station, the larger the size of the node. The edge direction is the direction of the riding flows between stations, and the width of the edge is proportional to the amount of flow. If there is a riding that starts and ends for the same station, there is a loop on the corresponding node. For instance, node 3 corresponding to station C has the highest number of flows. Node 1 and node 2 belong to a two-way connection, and each of them belongs to a one-way connection with node 3. Obviously, edge 3 between node 1 and node 3 has a larger flow than other edges. Edge 5 is a loop connecting the same node 2.

The above bike-sharing network provides a basic structure for subsequent data analysis. Using network analysis methods, a series of relevant indicators on the bike-sharing network can be identified and their analysis can be carried out to investigate the network characteristics from different perspectives.

The statistical analysis of the network in this study is dedicated to understanding the main characteristics of bike flow. Statistical indicators, such as node average flow and edge average flow of the whole network, can reflect general flow characteristics. By extracting and spatially visualizing edges with a large volume of flow in the bike-sharing network, we may analyze the spatial distribution characteristics of the main flow more intuitively. In particular, this study also focuses on extracting ridings at the same borrowing and return station, which often corresponds to leisure trips [45]. A particular interest of this study is to investigate how the pandemic affects leisure riding, and what changes take place in the spatial distribution of the main flow of leisure riding.

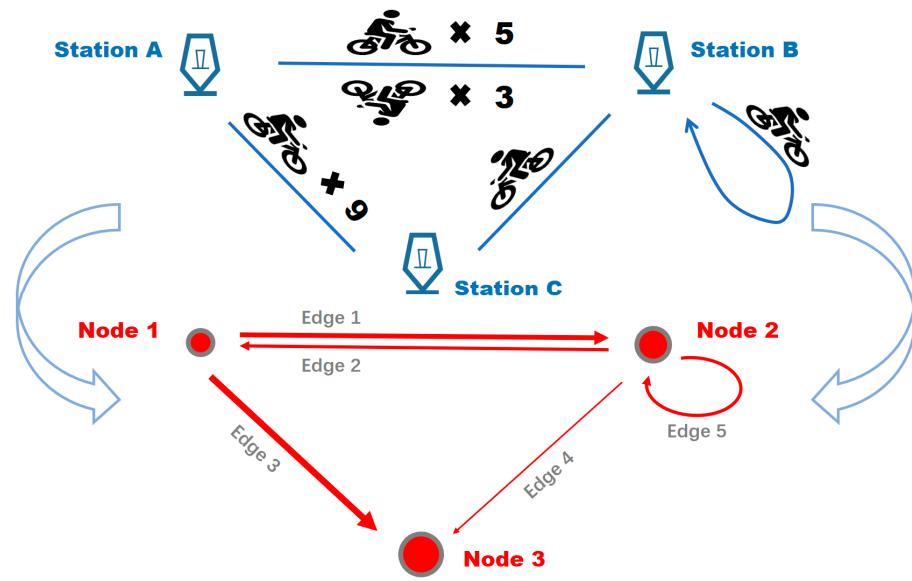


Figure 3. Network organization of riding data.

Formula (1) is introduced to calculate the variation coefficient of the flow, which reflects the dispersion degree of flow distribution in the bike-sharing network, and is not influenced by measurement scale and dimension; x is the flow value, σ and μ represent the standard deviation and the average value of the data. The average value is expressed in Formula (2), where x_i represents the flow of node i (or the flow of edge i), n is the number of nodes (or edges), and d is the number of days in the experimental data. For the bike-sharing network, the higher the $CV(x)$, the stronger the heterogeneity of the flow distribution, which means the flow distribution is more unbalanced.

$$CV(x) = \frac{\sigma(x)}{\mu(x)} \tag{1}$$

$$\sigma(x) = \frac{\sum_{i=1}^n x_i}{n \times d} \tag{2}$$

To further study the structure of the bike-sharing network and the impact of the pandemic on it, the aggregation indicators of the network are introduced, which may reflect the change in the aggregation degree of the bike-sharing network. In this study, the average aggregation coefficient and the global aggregation coefficient are used to investigate the network aggregation locally and globally, respectively.

The average aggregation coefficient is based on the local aggregation coefficient, which is calculated to measure the aggregation degree around each node. The local aggregation coefficient of a node is the ratio between the number of edges between its connected nodes and the number of possible edges between them. For node i , its local aggregation coefficient c_i is calculated according to Formula (3). If and only if there is a connection between node i and j , $a_{ij} = 1$, otherwise $a_{ij} = 0$, and k_i represents the degree of node i , $k_i^{*} = \sum_{i \neq j} a_{ij} a_{ji}$. By taking the average of the local aggregation coefficients of all nodes, we obtain the average aggregation coefficient of the network. In the bike-sharing network, a high average aggregation coefficient indicates that the stations are well connected with their surrounding stations and there is good local aggregation between these stations.

$$c_i = \frac{\sum_h \sum_j (a_{ij} + a_{ji})(a_{jh} + a_{hj})(a_{hi} + a_{ih})}{2[k_i(k_i - 1) - 2k_i^{*}]} \tag{3}$$

The definition of the global aggregation coefficient is based on the so-called node triples in the network. If three nodes are connected in pairs, they form a closed triple. If there are only two connecting edges between three nodes, they are called open triples. By counting the number of different types of triples in the network, the global aggregation coefficient is obtained as shown in Formula (4), where G_c is the number of closed triples in the network and G_o is the number of open triples. A bike-sharing network with a high global aggregation coefficient indicates a good network aggregation and a relatively saturated interconnection between stations.

$$C = \frac{3 \times G_c}{3 \times G_c + G_o} \quad (4)$$

4.2. OD Clustering of Bike-Sharing Data

Based on the constructed bike-sharing network above, we can summarize its basic flow statistics. A common way to extract the main riding flows is by directly filtering out the number of flows above a given threshold from the constructed bike-sharing network. However, this approach may ignore large groups of flows where individual edges may not have large flows, but they spatially and directionally close and together form a large flow connecting different regions. These groups can be a good description of the distribution of main flows with similar spatial patterns. To extract these edge groups of large flows, we apply an OD clustering method that considers multiple spatial factors and edge flow on the bike-sharing network. Unlike the idea of clustering by the location of starting points or end points, respectively, the OD clustering in this study considers the locations of both start points and end points. The general process is described below.

For any two edges E_i and E_j in the network, their spatial similarity is calculated as follows: $\langle O_i, D_i \rangle$ and $\langle O_j, D_j \rangle$ are the OD pairs of E_i and E_j , respectively. F_i and F_j are the riding flows on the two edges. We impose the distance constraint of OD data as shown in Figure 4. Taking O_i and D_i as the center points, and DI as the search radius, the two circles show the neighborhood of O_i and D_i . For any other edge in the network, if its origin and destination fall in the neighborhood of O_i and D_i , respectively, this edge meets the distance constraint conditions. From Figure 4, we can see that the purple line E_j fulfills this requirement, while the two green arrow lines are filtered out. The distance threshold is expressed in Formula (5), where $dist()$ is the distance calculation function to calculate the distance between the start points and the end points of the two edges.

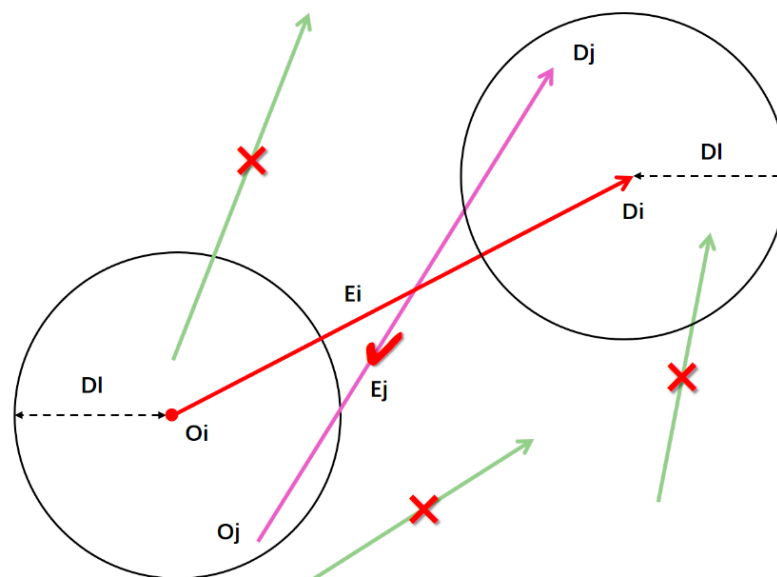


Figure 4. Spatial constraints for edge similarity determination.

$$\text{dist}(O_i, O_j) \leq DI \cap \text{dist}(D_i, D_j) \leq DI \quad (5)$$

However, using the distance constraint alone may not guarantee the spatial similarity of the two edges. As demonstrated in Figure 5, E_i or E_j are rather short and reveal large directional differences, even if O_j and D_j satisfy the distance constraint. Therefore, the angle constraint is introduced as shown in Formula (6) to assure the edges with smaller angles and consistent direction. The function of the angle threshold is expressed in Formula (6), in which $\text{Angle}()$ is the angle calculation function and AI is the angle threshold.

$$\text{Angle}(E_i, E_j) \leq AI \quad (6)$$

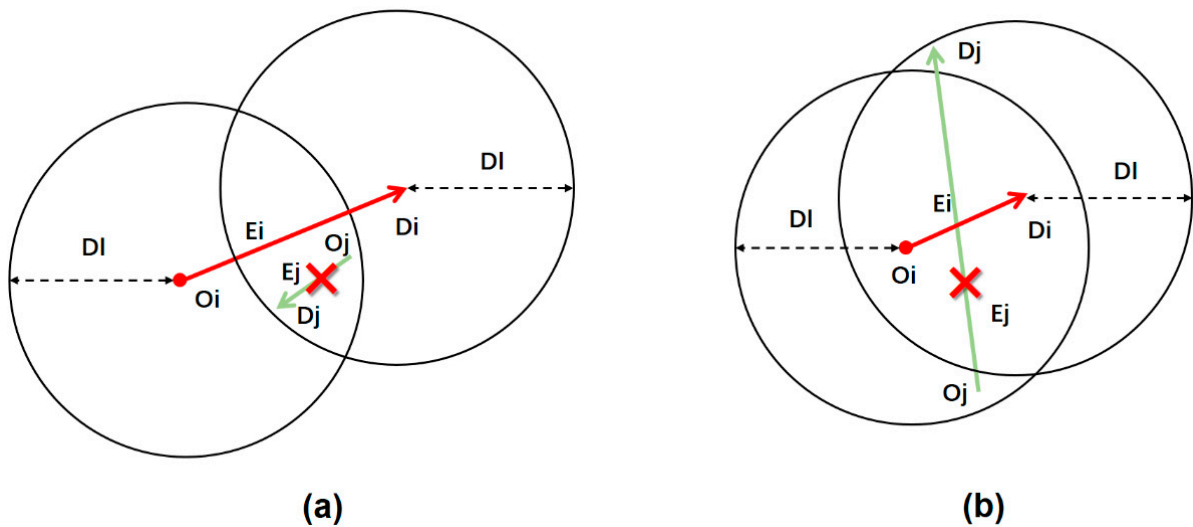


Figure 5. Using distance constraint alone cannot guarantee spatial similarity (a) Approximate opposite direction (b) Approximate orthogonal direction.

In cluster extraction, this study sets threshold constraints on both edge flow and the number of edges in the cluster. To take into account the edge flow in clustering, we use the threshold ft for edge flow to filter large flow edges in cluster extraction. Through threshold ft , only edges with a flow greater than ft can participate in clustering. In addition, the threshold for the number of edges in clustering is set to et to extract large flow edge groups. That means only clusters with more than et edges can be extracted as the final results. The clustering process runs as follows:

- (1) For an unprocessed edge E_i in the bike-sharing network, if its flow is greater than ft , execute step (2). Otherwise, mark it as processed and repeat step (1);
- (2) Calculate the distance and angle between E_i and the edge around it in $\{E_1, E_2, E_3 \dots \dots E_n\}$ with edge flow greater than ft . Select edges that satisfy the distance constraint in Formula (5) and the angle constraint in Formula (6) to form a group;
- (3) If the number of edges in the group in (2) is larger than et , it is identified as a cluster and go to step (4). Otherwise, mark E_i as processed and go to step (1);
- (4) The total flow of all edges in the cluster is calculated and recorded to edge E_i , which is marked as the core edge. All edges in the cluster are marked as processed. Go to step (1).

Figure 6 shows an example of a large flow edge cluster and its core edge. Finally, all the large flow edge clusters and their core edges are extracted.

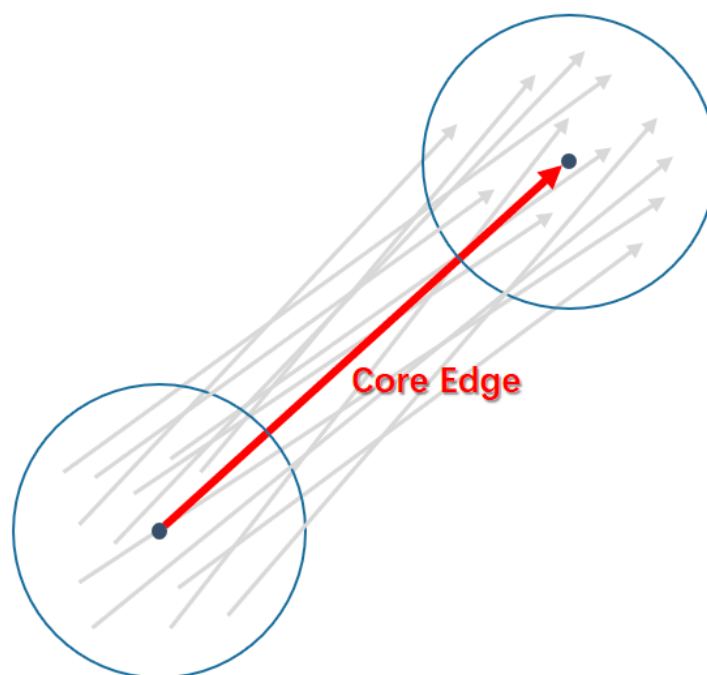


Figure 6. An edge cluster of a large flow and its core edge.

4.3. Extraction and Analysis of Rebalancing Data

The uneven spatial distribution of riding behavior leads to the imbalance of supply and demand of bikes and docks. This may make it difficult for users to find bikes or empty docks at the target station. Sometimes, bike-sharing companies may take corresponding measures to encourage users to borrow bikes from bike-rich stations near their starting points and return them at dock-rich stations near their destinations, which may facilitate a state of the self-balance system without external help [46]. However, at present, it is difficult to avoid the imbalance between the supply and demand of bikes and docks only relying on the self-balancing mechanism. Therefore, the rebalance operation is needed to solve the above problem. Good rebalance can meet the needs of bike use and return, ensure the stable operation of the bike-sharing system, and improve user satisfaction [44]. Meanwhile, the analysis of the collected rebalancing data can provide a new perspective for understanding the operation of bike-sharing systems.

Normally, riding data does not explicitly contain the rebalancing data, but we may derive the information using the following method: First, the riding data are grouped by the bike ID, and data with the same ID are sorted by their timestamps. As shown in Figure 7, for a bike with the corresponding ID, if there is no interruption, its spatial movement trajectory of different stations should be continuous, that is, the start station of the current data record should be consistent with the end station of the previous data record. If the spatial moving trajectory of a bike is interrupted, it can be inferred that a rebalancing operation took place at the interruption (red circle in Figure 7). The direction of the rebalancing is from the station before the interruption to the station after the interruption (station C to station D in Figure 7).

Therefore, the rebalancing data can be extracted from the riding data by detecting the interrupted segments of the riding trajectories. The rebalancing data are also typical OD data, which can be organized as the same data structure as the riding data. As shown in Figure 7, the start station of rebalancing is the station before the trajectory interruption (Station C), and the end station of rebalancing is the station after the trajectory interruption (Station D). The start time of rebalancing is the time when the bike returns to the station before the trajectory interruption (t_1), and the end time of rebalancing is the time when the bike leaves the station after the trajectory interruption (t_2).

The duration of rebalancing is the difference between the end time and the start time, which includes three components, i.e., the waiting time of the bike at the start station of rebalancing (d_1), the real rebalancing time by the company (d_2), and the waiting time of the bike at the end station of rebalancing (d_3). As shown in Figure 7, the duration of rebalancing is the total sum of d_1 , d_2 , and d_3 . Since the bike-rebalancing time (d_2) spent on transporting bikes is normally short, a longer rebalancing time indicates that the bike was potentially standing in the station for a long time before rebalancing, or/and the bike was potentially waiting at the station for a long time after rebalancing. Therefore, a long rebalancing duration has a poor description of the time distribution of rebalancing behavior. A short rebalancing duration indicates that the rebalancing operation happens immediately after the bike returns to the station and the bike is used immediately after the rebalancing, which reflects timely dispatching. In case of a short duration of rebalancing, both the start time and the end time of rebalancing can approximately describe the occurrence time of the rebalancing operation.

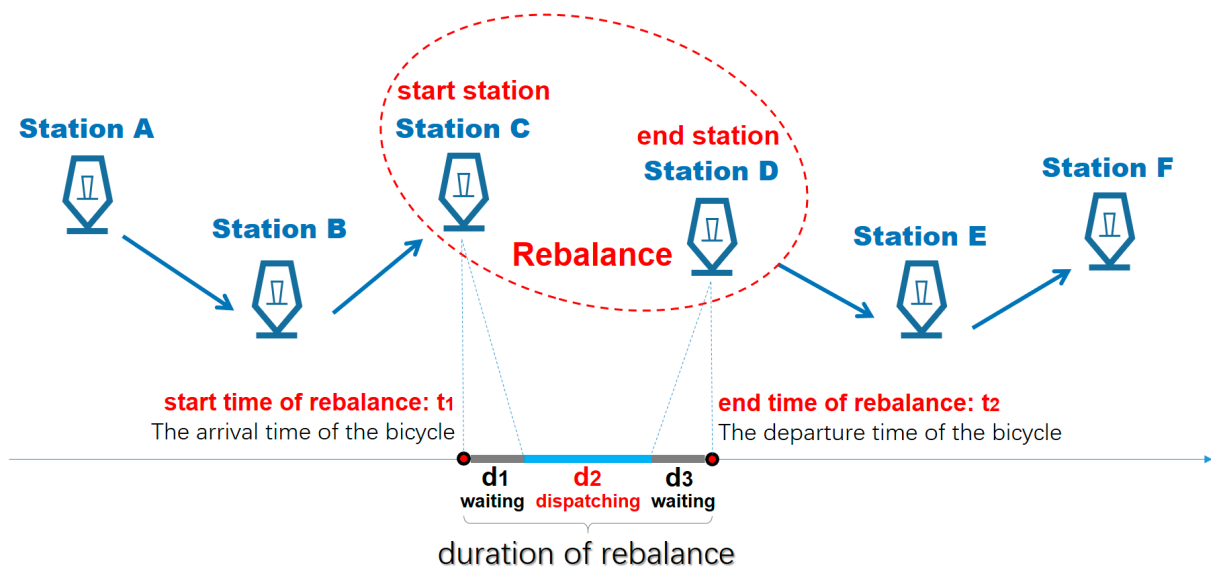


Figure 7. Detection of rebalancing behavior.

Note that the absolute number of the rebalancing operations cannot be directly used to describe the rebalancing efficiency, because generally, in a bike-sharing system, the larger the riding volume is, the larger the rebalance volume will be. Hence, we introduce the rebalancing ratio RR in Formula (7) as the ratio between the number of rebalancing operations RA and the total number of ridings TA . Furthermore, spatiotemporal analysis can be carried out based on the derived rebalancing data.

$$RR = \frac{RA}{TA} \quad (7)$$

5. Experiment and Analysis

5.1. Data Processing and Comprehensive Analysis

To investigate the changes in main flows in the bike-sharing system of our test area, we plot the monthly flow distributions in the pre-pandemic year of 2019 and the pandemic year of 2020. As shown in Figure 8, the monthly flow in 2019 exhibits a trend of first rising and then declining, reaching the peak in September. In 2020 there is a large difference at the early stage of the pandemic, reaching the valley in April, and afterward showing an upward mainly due to the good resilience of the bike-sharing system.

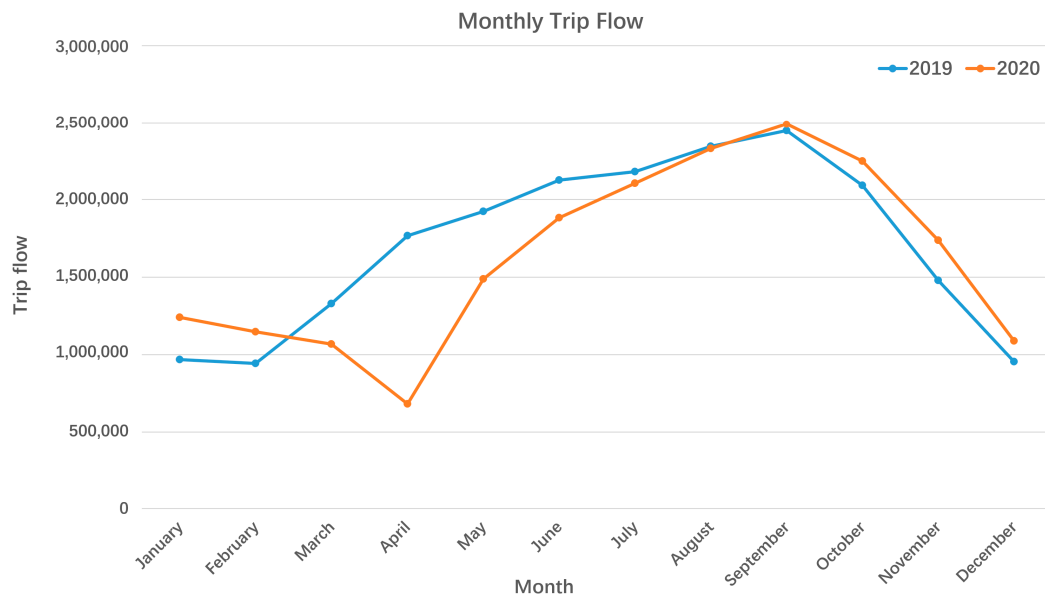


Figure 8. Monthly flows of the bike-sharing system in New York.

To study the impact of the pandemic on the main flows of the bike-sharing system, we focused on data from April, the month with the most drastic changes. We selected four Wednesdays in April of 2019 and 2020 for comparative analysis in the following experiments. We also checked the weather on these four days, which was not bad or extreme, such as heavy rain, and thus would not have significant influence on rides. We then constructed the bike-sharing networks based on these two data sets in 2019 and 2020, respectively, and visualized the networks in Figure 9. The black dots represent stations, and the lines between them are riding flows, with blue to red indicating the amount of flow from small to large. The large flow edges in the network are mainly located in Manhattan Island, and the number of large flow edges of the corresponding period in 2020 is much less than that in 2019. Figure 10 shows the frequency distribution of the edge flow in the network. There are a large number of edges with only one or two trips, and the edges with more than five trips are relatively large flow edges.

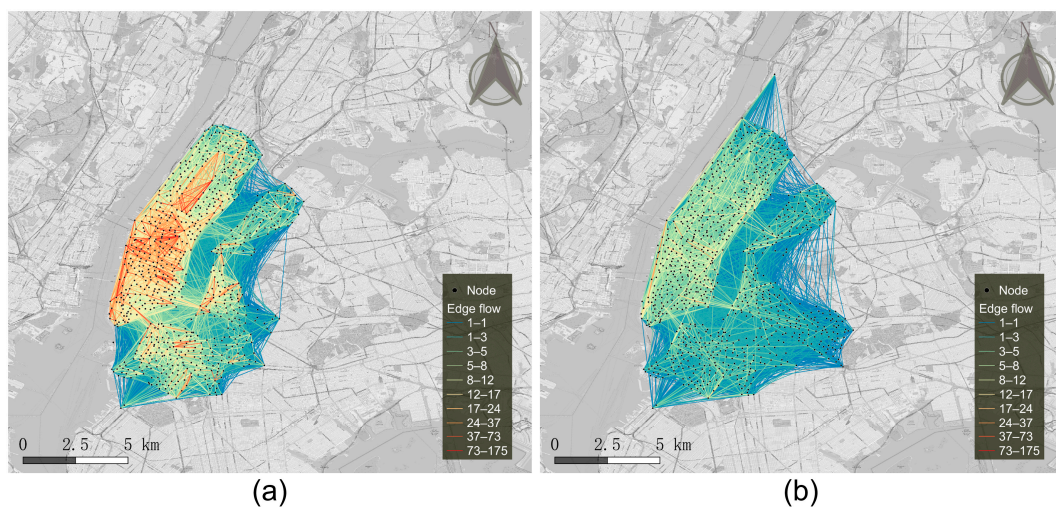


Figure 9. Bike-sharing networks of the first four Wednesdays in (a) 2019 and (b) 2020.

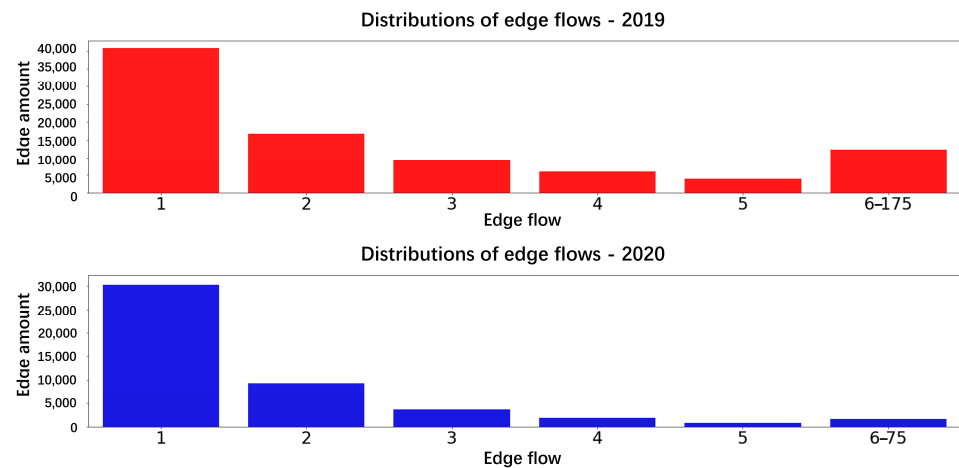


Figure 10. Statistical distributions of edge flows in two time periods of 2019 and 2020.

We further calculated the values of the network indicators mentioned in Section 4 for both data sets. The statistical results are shown in Table 2. In terms of average flow, both network node flow and network edge flow decreased significantly in the corresponding period of 2020 compared to that of 2019. However, the coefficient of variation in flows in 2020, especially the coefficient of variation in edge flows, is much smaller. This indicates that the distribution of riding flows in 2020 is less heterogeneous. Regarding the clustering degree, both the average aggregation coefficient and the global aggregation coefficient reflect a lower degree of clustering and a stronger dispersion of the bike-sharing network in the corresponding period of 2020. Based on the values of these indicators in two time periods, it roughly shows that during the initial stage of the pandemic, people substantially reduced travel, and there was a tendency to avoid gatherings.

Table 2. Statistical values of network indicators in two time periods of 2019 and 2020.

	2019	2020
Node average flow (/day)	177.54	45.11
Coefficient of variation in node flow	0.96	0.88
Edge average flow (/day)	0.78	0.43
Coefficient of variation in edge flow	1.37	0.85
Average aggregation coefficient	0.5	0.31
Global aggregation coefficient	0.53	0.34

5.2. Analysis of Large Flow Edges

We further conduct the macroscopic statistical analysis of large flow edges, which are divided into two types: self-loop station flows with the same start and end stations and inter-station flow groups with different start and end stations. We first derived several largest self-loop station flows. As shown in Table 3, the loops account for only a small portion in the corresponding period of 2019, with the proportions in the top 100, top 200, and top 300 large flow edges being 12%, 7.5%, and 7%, respectively. However, in the corresponding period of 2020, this type of edge accounts for most of the large flow edges with the proportions in the top 100, top 200, and top 300 large flow edges being 81%, 72%, and 67%, respectively. These differences suggest that the self-loop station flows increased significantly in large flow edges during the pandemic. According to Noland et al. (2016), ridings at the same borrowing and return station are mainly for leisure purposes. Thus, we may infer from the proportions that leisure riding increased in the corresponding period of 2020. Most prominently, among the top 100 edges of flow in 2020, the loops account for 81%. There might be two plausible reasons for this phenomenon. On the one hand, due to the government's lockdown policies, people were commuting less. The demand for riding, which was responsible for the last kilometer of commuting, was greatly weakened; on the

other hand, with the closure of public entertainment places, riding, which can avoid contact in enclosed spaces, became a viable form of recreation during the period of isolation.

Table 3. The proportion of the loops in top flow edges in two time periods of 2019 and 2020.

	Top Flow Edges	Number of Loops	Loop Proportion
2019	Top 100	12	12%
	Top 200	15	7.5%
	Top 300	21	7%
2020	Top 100	81	81%
	Top 200	144	72%
	Top 300	201	67%

To further observe the spatial distribution of the self-loop station flows, we extracted and visualized 20 riding stations with the largest flows of two data sets, respectively, on the map. As shown in Figure 11, most of these riding stations are located near parks, riverbanks, and other outdoor leisure sites. In the overall spatial distribution, as shown in Figure 11a, there is an obvious localized clustering of such stations in 2019, with the most prominent place being Central Park, where 9 of the top 20 stations with the largest flows are located. In 2020, the distribution of such stations is relatively scattered, and the phenomenon of localized clustering is not as obvious. There are only four stations around Central Park (Figure 11b). This is consistent with the phenomenon that the network aggregation degree is reduced due to the impact of the pandemic. It can be speculated that during the pandemic, people's leisure riding reflected the avoidance of gatherings. For instance, in areas with frequent riding activities in the past, such as Central Park, the large flows of leisure ridings decreased significantly. The number of top self-loop flow stations increased in Manhattan during the pandemic. As shown in Figure 11, there are 13 top flow self-loop stations in Manhattan in the corresponding period of 2019. However, in 2020 this number became 16. In both years, many stations of this type are distributed along the river bank.

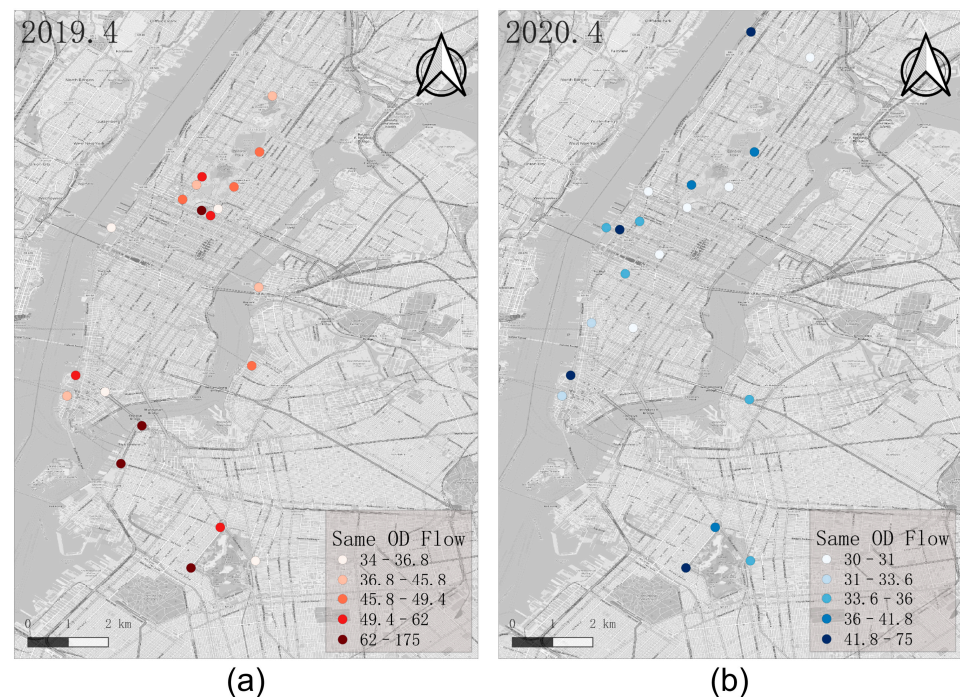


Figure 11. Twenty stations of largest flows with the same start and end stations (a) stations in 2019.4 (b) stations in 2020.4.

Moreover, we extracted the top 20 inter-station flow edges in corresponding periods of both years. As shown in Figure 12, compared with 2019, the amount of flow in 2020 decreased significantly. In terms of spatial distribution, the distribution range of these large flow edges in 2020 was also reduced, and they were only distributed in the Manhattan area. There were many large flow edges near Central Park in 2019. However, they disappeared in this area in 2020 and instead, they were concentrated near the West Bank of Manhattan. This phenomenon is similar to the high self-loop station riding flows, which further confirms the avoidance of gatherings during the pandemic.

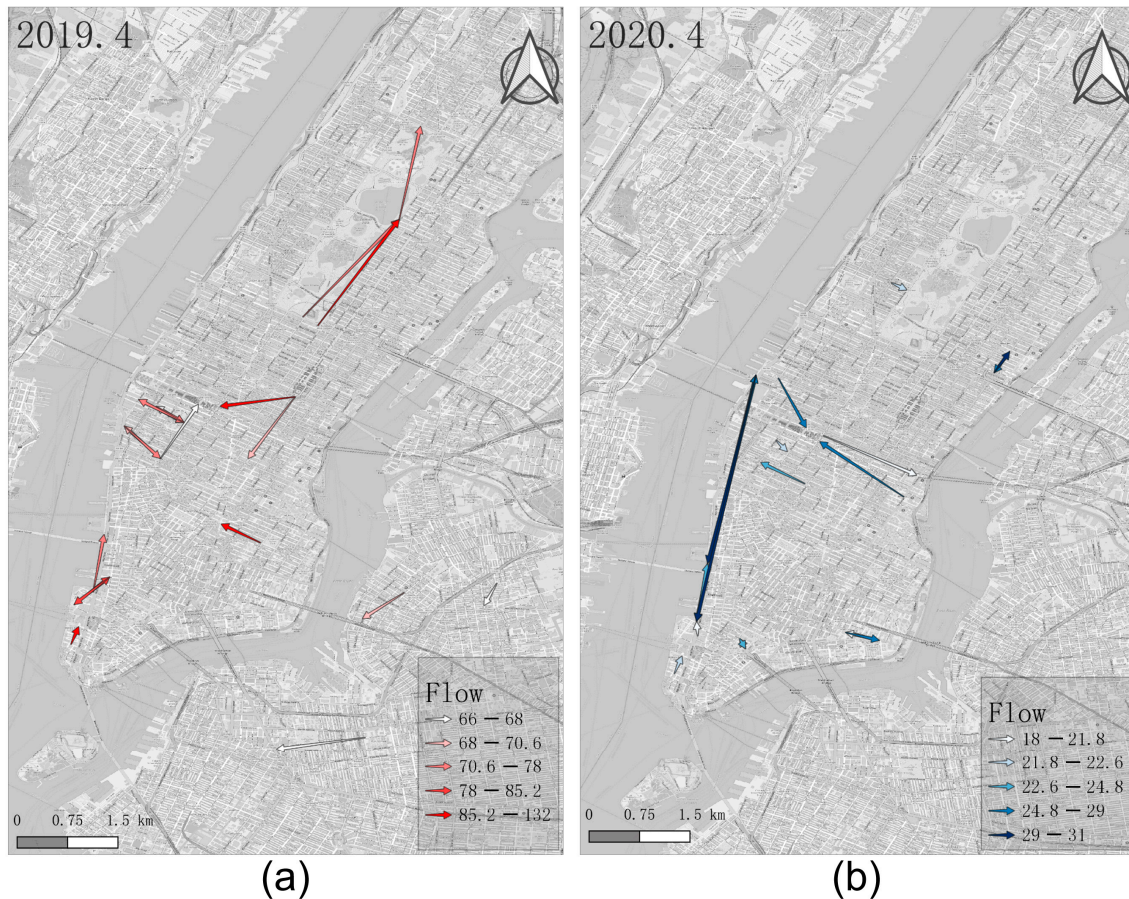


Figure 12. Top 20 flow edges of different start and end stations (a) Edges in 2019.4 (b) Edges in 2020.4.

5.3. Analysis of Large Flow Edge Group

We cluster the large flows according to the method proposed in Section 4.2. This method requires two parameters, i.e., the threshold of ft for edge flow and the threshold et for the number of edges. We set ft to 5 based on the flow statistics. In the two time periods of 2019 and 2020, there are 12,312 and 1608 edges with flows larger than 5, respectively. Regarding the setting of the threshold et , due to the large difference in the amount of the data between these two time periods, we use the ratio r , i.e., the ratio of the number of large flow edges of two data sets when setting et . As the total number of flows in the corresponding period of 2020 is very small, we use its et as a basis and set it to 5, 10, and 15, respectively. Based on the et values for 2020, we calculated the corresponding values in 2019 as 38, 77, and 115, which are the products of r and the et values for 2020. Many studies confirmed that 1km is a common service range for urban bike-sharing [47,48]. Therefore, the search radius Dl in this study is set to 1 km. The angle threshold Al is set to 30° to ensure that the direction difference of edges in the cluster is not large.

We visualized the spatial distribution of clustering results represented by core edges (i.e., the aggregated flows on the core edges) on the map. As shown in Figure 13, the

upper row shows the clustered flows in 2019 with three et values of 115 (Figure 13(a1)), 77 (Figure 13(a2)), and 38 (Figure 13(a3)), while the lower row shows the clustered flows in 2020 with three et values of 15 (Figure 13(b1)), 10 (Figure 13(b2)), and 5 (Figure 13(b3)). We can see that the core edges of clustering are mainly concentrated in the connection area of midtown and downtown Manhattan when et is larger in 2019 (Figure 13(a1)). With the decrease in et , the extent of core edges spreads from the center to the periphery, and gradually extends to cover the midtown and downtown (Figure 13(a2,a3)). When et is larger in 2020, the extent of the core edges is not concentrated and is mainly distributed in the connecting area of midtown and downtown and the east riverbank of Manhattan (Figure 13(b1)). With the decrease in et , the trend is not similar to 2019. In Figure 13(b2,b3), we can see that the core edges increased mostly along the riverbank of Manhattan, while in the central area, it is largely missing. The results suggest that the spatial distribution of the large flow edge groups became more dispersed during the initial stage of the pandemic with the central aggregation pattern of 2019 disappearing, and the distribution along the river was more obvious.

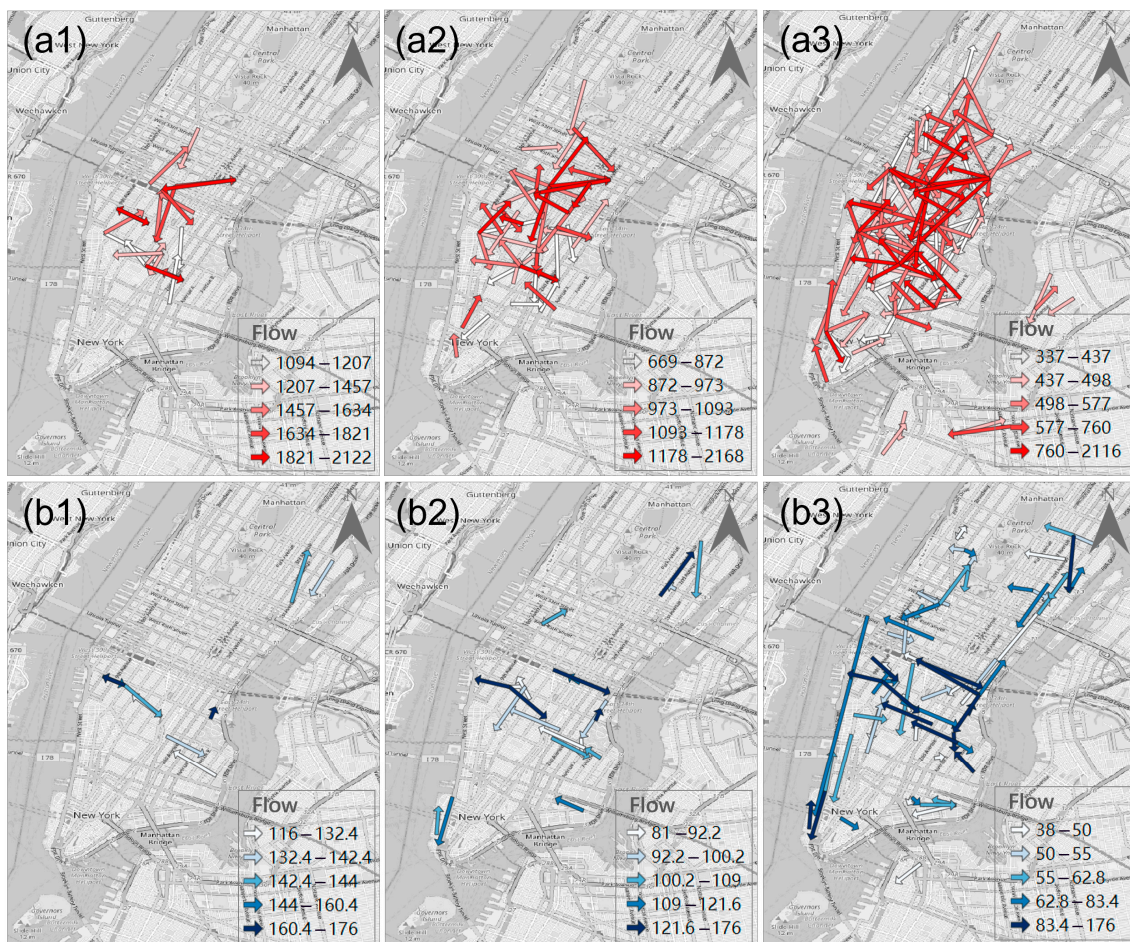


Figure 13. The clustering results of different et represented by core edges (a1) 2019 $et = 115$; (a2) 2019 $et = 77$; (a3) 2019 $et = 38$; (b1) 2020 $et = 15$; (b2) 2020 $et = 10$; and (b3) 2020 $et = 5$.

5.4. Analysis of Rebalancing Data

The rebalancing data were extracted from the data in 2019 and 2020, respectively, to analyze the distribution of the rebalancing behavior. As introduced in Section 4.3, the rebalancing duration has three components, i.e., the waiting time at the start station of rebalance, the real rebalancing time by the company, and the waiting time at the end station of rebalance. To improve the description accuracy of the rebalancing occurrence time, we

chose data with a rebalancing duration less than 10 min, which might describe the real rebalancing time by the company, and used the end time of rebalancing for the analysis. The distribution of rebalancing time is shown in Figure 14. Obviously, the rebalancing in 2019 has two main peaks in the morning and evening, which correspond well to work commuting times. This indicates that the use of shared bikes for commuting in the city affects the supply and demand balance of bikes and docks. Timely rebalancing is needed to meet commuting demand and maintain the stability of the system. Unlike in 2019, the peak time of rebalancing during the pandemic period in 2020 is around 3 p.m. Due to the lockdown policies during the pandemic, people worked mainly at home, and their demand for commuting was weakened. Instead, the demand for safe leisure increased. A large number of leisure rides in the afternoon triggered a new peak of rebalancing.

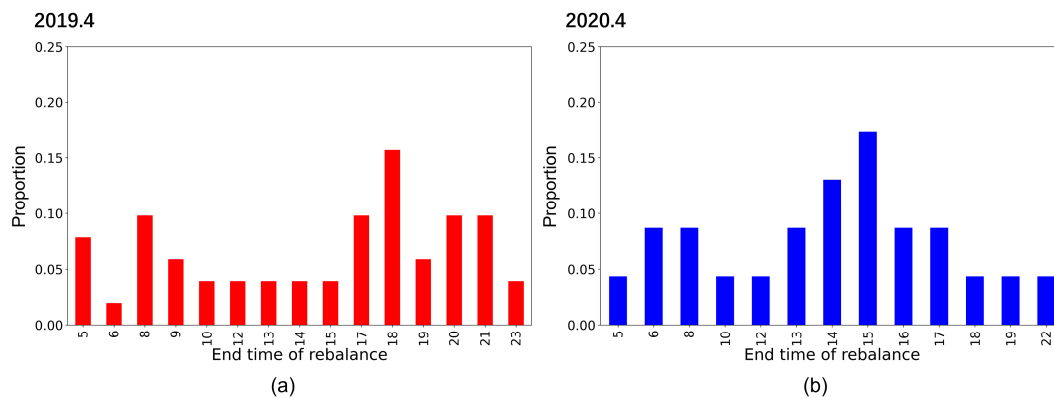


Figure 14. Statistics of the end time of rebalancing (rebalancing duration less than 10 min) (a) Statistics in 2019.4 (b) Statistics in 2020.4.

We further calculated the average number of daily rebalances and the average daily riding amount and their ratios for analysis. As shown in Table 4, the average number of rebalances in 2020 is lower than that in 2019 due to the decline of overall bike-sharing, but the ratio of the average number of rebalances to the average daily riding amount in 2020 is much higher than that in 2019. One possible reason is due to the large proportion of bikes borrowed from and returned to the same stations in 2020 (see Table 3). For the same station, a large number of borrowed bikes will result in a shortage of bikes, which would need a timely adjustment. When a large number of borrowed bikes from this station is returned, there will be a shortage of empty docks, which will need a timely adjustment too. If this situation continues, it may lead to the rise of the rebalancing ratio.

Table 4. Statistics of rebalancing times.

	Average Number of Rebalancing/day	Average Riding Amount/day	Rebalance Ratio
2019	7257.75	70,462.25	0.103
2020	4273.5	21769.5	0.1963

To further investigate the spatial distribution of rebalancing, we extracted the top 50 stations with the highest transfer volume as shown in Figure 15. Most of these stations are also distributed on Manhattan Island, especially in the middle and lower regions. Overall, the spatial distribution of top transfer in and out stations is relatively consistent. The results may indicate that the timely rebalancing of shared bikes is also constrained by the first law of geography and generally occurs between adjacent stations. In 2019, some of the top stations reveal a certain aggregation, as shown by the red circles in Figure 15. In 2020, the distribution of top transfer stations is more dispersed. These differences may be related to the more homogeneous flow distribution during the pandemic. People's rides

tend to avoid aggregation, thus reducing the imbalance of local bikes or docks caused by the large flow aggregation, resulting in a more balanced distribution of the top transfer stations.

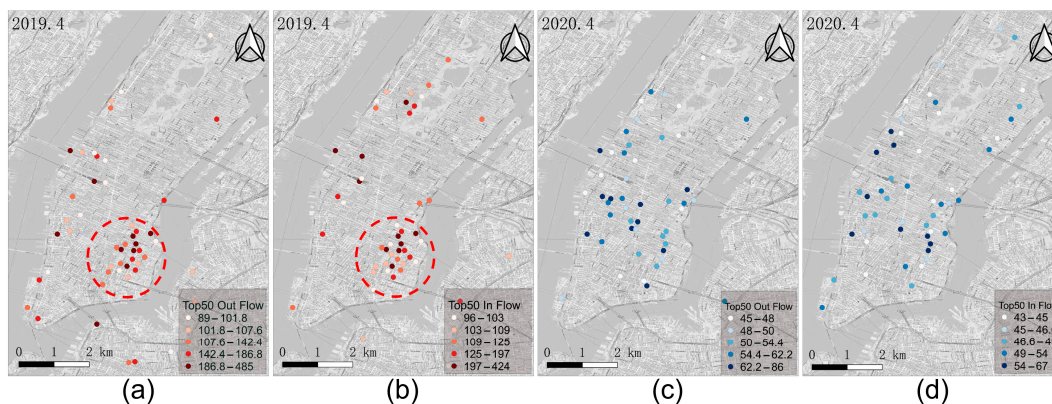


Figure 15. Top 50 stations with the highest transfer volume (a) Top 50 out flow stations in 2019.4 (b) Top 50 in flow stations in 2019.4 (c) Top 50 out flow stations in 2020.4 (d) Top 50 in flow stations in 2020.4.

6. Discussion

6.1. Study Results and Their Significance

This study explores the spatiotemporal variations of riding and rebalance of shared bikes before and during the pandemic for a better understanding of the impact of the pandemic on bike-sharing. The main findings are as follows:

- (1) The riding flows and their distribution during the pandemic changed significantly. On the one hand, there was a substantial reduction in network flow. On the other hand, compared with aggregated distributions in pre-pandemic times, the network flow was more evenly distributed and the aggregation of network connections was reduced in the early stage of the pandemic.
- (2) The proportion of high flow associated with self-loops at the stations increased significantly during the pandemic. In the pre-pandemic period, these stations were mostly concentrated in urban gathering places, such as Central Park. During the pandemic period, these stations were mostly scattered along the riverbanks. The distribution of large flow inter-station edges during the pandemic narrowed from the entire study area to Manhattan, and moved from the central area to the edge area.
- (3) In terms of large flow edge clusters, their spatial distribution changed significantly during the pandemic. Large flow edge clusters were more concentrated in prosperous areas in pre-pandemic times. However, during the pandemic period, the distribution of these clusters was more scattered and presented the characteristics of decentralization.
- (4) In terms of rebalancing, the peak of timely rebalancing shifted from two commuting peaks in the pre-pandemic period to one peak in the afternoon during the early stage of the pandemic. The number of rebalancing operations in the early stage of the pandemic decreased significantly, but the ratio between the number of rebalancing and the total number of ridings increased significantly. By analyzing stations with the highest number of rebalancing, we found that such stations showed a certain spatial aggregation during the pre-pandemic period, while the spatial distribution was more dispersed during the pandemic.

Our research results could provide reference and assistance in decision making for different user groups during the pandemic, such as travel planning for citizens, operation scheme optimization for bike-sharing companies, and overall management of the government. For citizens, reduced trip flow and more dispersed riding distribution are beneficial for infection prevention and control during a pandemic. Riding activities take

place in open spaces at a relatively safe distance, and their leisure function also provides a relatively healthy form of exercise for isolated living. Riding to medical treatment can also avoid, to some extent, close contact and virus transmission in the enclosed spaces of public transport. For bike-sharing companies, the more even riding flow distribution does not result in a good self-balancing system, with rebalancing demand becoming more dispersed and rebalancing rates increasing significantly. These problems challenge the company's operations. Current rebalancing routes and strategies should be reconsidered to ensure that they can meet the special needs of this period. For the government, the spatiotemporal changes in main riding flows could provide a reference for policy-making during the pandemic, such as residents' travel guidance and municipal service planning. Timely bike flow information disclosure could help residents avoid riding aggregation and reduce infection. In addition, the disinfection work should be further strengthened at the stations connected with the main flow.

Riding, which integrates commuting, leisure, and medical treatment during special periods, has great potential for application and may also provide useful assistance to urban recovery in the later stages of a pandemic. Considering that life in many places, including New York, is gradually returning to normal, our results can be used for reference in the following aspects: First, avoiding gathering riding is still an effective way to reduce infection and for self-protection when COVID-19 is not completely disappeared. Second, the leisure function of bikes provided an important mode of entertainment for people's lives during the pandemic, which is worth continuing and promoting in the post-pandemic era. Last but not least, shared bike riding undertook many new tasks during the pandemic, the development and maintenance of people's riding habits will be conducive to carbon emission reduction and environmental protection, and beneficial to sustainable life.

6.2. Limitations and Future Work

There are still some limitations in the current research, which need further studies. For instance, our research only focuses on the bike-sharing system, and especially the spatiotemporal variation characteristics of the main flows of bike-sharing. In the future, multiple transportation modes, such as subways, buses, and taxi cabs can be integrated to provide a more comprehensive understanding of people's mobility behavior during the pandemic. In addition to pure mobility data, other types of data, such as pandemic data, land use data, and demographic data could be integrated to achieve more in-depth analysis. As a global pandemic, COVID-19 affected people's lives around the world. The comparative study of mobility in different cities around the world supported by multi-source data can provide the differences in human activities affected by the pandemic in different places, policies, and cultural backgrounds, which is beneficial to understanding the global impact of the pandemic. This is also our future research direction.

7. Conclusions

This paper studies the spatiotemporal change patterns hidden in bike-sharing data during the COVID-19 pandemic. A combination of geospatial network analysis and OD clustering methods was used to analyze the data sampled in New York City. The main contributions of this study are as follows: In terms of research method, we propose a combination method that can obtain the macro analysis indicators and detailed visualization results. The mutually verified results not only enhance the reliability of the results, but also prove the effectiveness of the method. In terms of the research object, we not only analyze the bike-sharing trip data, but also extract and mine the rebalancing data together. This provides a new idea for the analysis of bike-sharing data in the future. In terms of research results, it reveals several interesting patterns and answers the questions raised in this study. The spatiotemporal patterns of the main flows of both riding and rebalancing were significantly affected by the pandemic. The pandemic not only significantly weakened the bike-sharing flows, but also made the distribution of main flows more discrete, and their uses are diverse; their recreational uses are especially more prominent. The rebalancing

rate increased during the pandemic, and the spatiotemporal patterns of rebalancing were also affected.

Author Contributions: Conceptualization, Rui Xin; Formal analysis, Linfang Ding, Bo Ai, Min Yang and Bin Cao; funding acquisition, Min Yang; methodology, Rui Xin, Bo Ai, Min Yang and Ruoxin Zhu; supervision, Liqiu Meng; visualization, Bin Cao; writing—review and editing, Linfang Ding and Liqiu Meng. All authors have read and agreed to the published version of the manuscript.

Funding: This research was funded by the National Natural Science Foundation of China (Grant No. 42101452; Grant No. 41871377), and the Natural Science Foundation of Shandong Province (Grant No. ZR2021QD027).

Institutional Review Board Statement: Not applicable.

Informed Consent Statement: Not applicable.

Data Availability Statement: The data that support the findings of this study are available in the public domain <https://ride.citibikenyc.com/system-data> (accessed on 6 January 2023). The base maps used in this paper are from OpenStreetMap.

Conflicts of Interest: The authors declare no conflict of interest.

References

- Nicola, M.; Alsafi, Z.; Sohrabi, C.; Kerwan, A.; Al-Jabir, A.; Iosifidis, C.; Agha, R. The socio-economic implications of the coronavirus and COVID-19 pandemic: A review. *Int. J. Surg.* **2020**, *78*, 185–193. [CrossRef] [PubMed]
- Greer, S.L.; King, E.; Massard da Fonseca, E.; Peralta-Santos, A. *Coronavirus Politics: The Comparative Politics and Policy of COVID-19*; University of Michigan Press: Ann Arbor, MI, USA, 2021.
- Arora, S.; Bhaukhandi, K.D.; Mishra, P.K. Coronavirus lockdown helped the environment to bounce back. *Sci. Total Environ.* **2020**, *742*, 140573. [CrossRef] [PubMed]
- Si, H.; Shi, J.G.; Wu, G.; Chen, J.; Zhao, X. Mapping the bike sharing research published from 2010 to 2018: A scientometric review. *J. Clean. Prod.* **2019**, *213*, 415–427. [CrossRef]
- Sun, Z.; Wang, Y.; Zhou, H.; Jiao, J.; Overstreet, R.E. Travel behaviours, user characteristics, and social-economic impacts of shared transportation: A comprehensive review. *Int. J. Logist. Res. Appl.* **2021**, *24*, 51–78. [CrossRef]
- Campisi, T.; Ali, N.; Akgün-Tanbay, N.; Canale, A.; Tesoriere, G. The development of electric 2 and 3-Wheelers for low carbon passenger transport: A long-term benefits assessment. In Proceedings of the AIP Conference Proceedings, Volzhsky, Russia, 13–17 November 2022; AIP Publishing LLC: Melville, NY, USA, 2022; Volume 2611, p. 060003.
- Fishman, E. Bikeshare: A review of recent literature. *Transp. Rev.* **2016**, *36*, 92–113. [CrossRef]
- Eren, E.; Uz, V.E. A review on bike-sharing: The factors affecting bike-sharing demand. *Sustain. Cities Soc.* **2020**, *54*, 101882. [CrossRef]
- Hu, S.; Xiong, C.; Liu, Z.; Zhang, L. Examining spatiotemporal changing patterns of bike-sharing usage during COVID-19 pandemic. *J. Transp. Geogr.* **2021**, *91*, 102997. [CrossRef]
- Pase, F.; Chiariotti, F.; Zanella, A.; Zorzi, M. Bike Sharing and Urban Mobility in a Post-Pandemic World. *IEEE Access* **2020**, *8*, 187291–187306. [CrossRef]
- Xin, R.; Ai, T.; Ding, L.; Zhu, R.; Meng, L. Impact of the COVID-19 pandemic on urban human mobility—A multiscale geospatial network analysis using New York bike-sharing data. *Cities* **2022**, *126*, 103677. [CrossRef]
- Jiao, J.; Lee, H.K.; Choi, S.J. Impacts of COVID-19 on bike-sharing usages in Seoul, South Korea. *Cities* **2022**, *130*, 103849. [CrossRef]
- Kim, M.; Cho, G.H. Examining the causal relationship between bike-share and public transit in response to the COVID-19 pandemic. *Cities* **2022**, *131*, 104024. [CrossRef] [PubMed]
- Nikiforiadis, A.; Ayfantopoulou, G.; Stamelou, A. Assessing the Impact of COVID-19 on Bike-Sharing Usage: The Case of Thessaloniki, Greece. *Sustainability* **2020**, *12*, 8215. [CrossRef]
- Gao, Y.; Li, T.; Wang, S.; Jeong, M.H.; Soltani, K. A multidimensional spatial scan statistics approach to movement pattern comparison. *Int. J. Geogr. Inf. Sci.* **2018**, *32*, 1304–1325. [CrossRef]
- Song, C.; Pei, T.; Ma, T.; Du, Y.; Shu, H.; Guo, S.; Fan, Z. Detecting arbitrarily shaped clusters in origin-destination flows using ant colony optimization. *Int. J. Geogr. Inf. Sci.* **2019**, *33*, 134–154. [CrossRef]
- He, B.; Zhang, Y.; Chen, Y.; Gu, Z. A simple line clustering method for spatial analysis with origin-destination data and its application to bike-sharing movement data. *ISPRS Int. J. Geo-Inf.* **2018**, *7*, 203. [CrossRef]
- Raviv, T.; Tzur, M.; Forma, I.A. Static repositioning in a bike-sharing system: Models and solution approaches. *EURO J. Transp. Logist.* **2013**, *2*, 187–229. [CrossRef]
- Pal, A.; Zhang, Y. Free-floating bike sharing: Solving real-life large-scale static rebalancing problems. *Transp. Res. Part C Emerg. Technol.* **2017**, *80*, 92–116. [CrossRef]

20. Buckee, C.O.; Balsari, S.; Chan, J.; Crosas, M.; Dominici, F.; Gasser, U.; Schroeder, A. Aggregated mobility data could help fight COVID-19. *Science* **2020**, *368*, 145–146. [CrossRef]
21. Sirkeci, I.; Yucesahin, M.M. Coronavirus and migration: Analysis of human mobility and the spread of COVID-19. *Migr. Lett.* **2020**, *17*, 379–398. [CrossRef]
22. König, A.; Dreßler, A. A mixed-methods analysis of mobility behavior changes in the COVID-19 era in a rural case study. *Eur. Transp. Res. Rev.* **2021**, *13*, 1–13. [CrossRef]
23. Bohman, H.; Ryan, J.; Stjernborg, V.; Nilsson, D. A study of changes in everyday mobility during the Covid-19 pandemic: As perceived by people living in Malmö, Sweden. *Transp. Policy* **2021**, *106*, 109–119. [CrossRef] [PubMed]
24. Tanveer, H.; Balz, T.; Cigna, F.; Tapete, D. Monitoring 2011–2020 Traffic Patterns in Wuhan (China) with COSMO-SkyMed SAR, Amidst the 7th CISM Military World Games and COVID-19 Outbreak. *Remote Sens.* **2020**, *12*, 1636. [CrossRef]
25. Liu, Q.; Sha, D.; Liu, W.; Houser, P.; Zhang, L.; Hou, R.; Yang, C. Spatiotemporal patterns of COVID-19 impact on human activities and environment in mainland China using nighttime light and air quality data. *Remote Sens.* **2020**, *12*, 1576.
26. Willberg, E.; Järv, O.; Väisänen, T.; Toivonen, T. Escaping from cities during the covid-19 crisis: Using mobile phone data to trace mobility in finland. *ISPRS Int. J. Geo-Inf.* **2021**, *10*, 103. [CrossRef]
27. Li, Z.; Huang, X.; Zhang, J.; Zeng, C.; Olatosi, B.; Li, X.; Weissman, S. Human Mobility, Policy, and COVID-19: A Preliminary Study of South Carolina. 2020. Available online: http://gis.cas.sc.edu/gibd/wp-content/uploads/2021/01/HumanMobility_SC_preprint.pdf (accessed on 6 January 2023).
28. Noland, R.B. Mobility and the effective reproduction rate of COVID-19. *J. Transp. Health* **2021**, *20*, 101016.
29. Wang, H.; Noland, R.B. Bikeshare and subway ridership changes during the COVID-19 pandemic in New York City. *Transp. Policy* **2021**, *106*, 262–270. [CrossRef]
30. Shaheen, S.A.; Guzman, S.; Zhang, H. Bikesharing in Europe, the Americas, and Asia: Past, present, and future. *Transp. Res. Rec.* **2010**, *2143*, 159–167. [CrossRef]
31. Fishman, E.; Washington, S.; Haworth, N. Bike share: A synthesis of the literature. *Transp. Rev.* **2013**, *33*, 148–165. [CrossRef]
32. Chai, X.; Guo, X.; Xiao, J.; Jiang, J. Spatiotemporal analysis of share bike usage during the COVID-19 pandemic: A case study of Beijing. *arXiv* **2020**, arXiv:2004.12340.
33. Teixeira, J.F.; Lopes, M. The link between bike sharing and subway use during the COVID-19 pandemic: The case-study of New York's Citi Bike. *Transp. Res. Interdiscip. Perspect.* **2020**, *6*, 100166. [CrossRef]
34. Bucsky, P. Modal share changes due to COVID-19: The case of Budapest. *Transp. Res. Interdiscip. Perspect.* **2020**, *8*, 100141. [CrossRef] [PubMed]
35. Padmanabhan, V.; Penmetsa, P.; Li, X.; Dhondia, F.; Dhondia, S.; Parrish, A. COVID-19 effects on shared-biking in New York, Boston, and Chicago. *Transp. Res. Interdiscip. Perspect.* **2021**, *9*, 100282. [CrossRef] [PubMed]
36. Nikitas, A.; Tsigdinos, S.; Karolemeas, C.; Kourmpa, E.; Bakogiannis, E. Cycling in the Era of COVID-19: Lessons Learnt and Best Practice Policy Recommendations for a More Bike-Centric Future. *Sustainability* **2021**, *13*, 4620. [CrossRef]
37. Jobe, J.; Griffin, G.P. Bike share responses to COVID-19. *Transp. Res. Interdiscip. Perspect.* **2021**, *10*, 100353. [CrossRef]
38. Büchel, B.; Marra, A.D.; Corman, F. COVID-19 as a window of opportunity for cycling: Evidence from the first wave. *Transp. Policy* **2022**, *116*, 144–156. [CrossRef]
39. Kraus, S.; Koch, N. Provisional COVID-19 infrastructure induces large, rapid increases in cycling. *Proc. Natl. Acad. Sci. USA* **2021**, *118*, e2024399118. [CrossRef]
40. Wang, Y.; Szeto, W.Y. Static green repositioning in bike sharing systems with broken bikes. *Transp. Res. Part D Transp. Environ.* **2018**, *65*, 438–457. [CrossRef]
41. Cruz, F.; Subramanian, A.; Bruck, B.P.; Iori, M. A heuristic algorithm for a single vehicle static bike sharing rebalancing problem. *Comput. Oper. Res.* **2017**, *79*, 19–33. [CrossRef]
42. Ho, S.C.; Szeto, W.Y. A hybrid large neighborhood search for the static multi-vehicle bike-repositioning problem. *Transp. Res. Part B Methodol.* **2017**, *95*, 340–363. [CrossRef]
43. Ghosh, S.; Varakantham, P.; Adulyasak, Y.; Jaillet, P. Dynamic repositioning to reduce lost demand in bike sharing systems. *J. Artif. Intell. Res.* **2017**, *58*, 387–430. [CrossRef]
44. Caggiani, L.; Camporeale, R.; Ottomanelli, M.; Szeto, W.Y. A modeling framework for the dynamic management of free-floating bike-sharing systems. *Transp. Res. Part C Emerg. Technol.* **2018**, *87*, 159–182. [CrossRef]
45. Noland, R.B.; Smart, M.J.; Guo, Z. Bikeshare trip generation in New York city. *Transp. Res. Part A Policy Pract.* **2016**, *94*, 164–181. [CrossRef]
46. Tedeschi, A. Rebalancing Citi Bike: A Geospatial Analysis of Bike Share Redistribution in New York City. Doctoral dissertation, Universidade Nova de Lisboa, Lisbon, Portugal, 2016.

47. Yang, Y.; Heppenstall, A.; Turner, A.; Comber, A. A spatiotemporal and graph-based analysis of dockless bike sharing patterns to understand urban flows over the last mile. *Comput. Environ. Urban Syst.* **2019**, *77*, 101361. [[CrossRef](#)]
48. Ye, M.; Chen, Y.; Yang, G.; Wang, B.; Hu, Q. Mixed logit models for travelers' mode shifting considering bike-sharing. *Sustainability* **2020**, *12*, 2081. [[CrossRef](#)]

Disclaimer/Publisher's Note: The statements, opinions and data contained in all publications are solely those of the individual author(s) and contributor(s) and not of MDPI and/or the editor(s). MDPI and/or the editor(s) disclaim responsibility for any injury to people or property resulting from any ideas, methods, instructions or products referred to in the content.